BAP1 forms a trimer with HMGB1 and HDAC1 that modulates gene × environment interaction with asbestos

Flavia Novelli[a,1], Angela Bononi[a,1], Qian Wang[b,c], Fang Bai[b], Simone Patergnani[d], Franz Kricek[e], Ellinor Haglund[f], Joelle S. Suarez[a], Mika Tanji[a], Ronghui Xu[a], Yasutaka Takanishi[a], Michael Minaai[a], Sandra Pastorino[a], Paul Morris[a], Greg Sakamoto[a], Harvey I. Pass[g], Haithem Barbour[h], Giovanni Gaudino[a], Carlotta Giorgi[d], Paolo Pinton[d], Jose N. Onuchic[b], Haining Yang[a,2], and Michele Carbone[a,2]

[a]Thoracic Oncology, University of Hawaii Cancer Center, Honolulu, HI 96816; [b]Center for Theoretical Biological Physics, Rice University, Houston, TX 77005; [c]Hefei National Laboratory for Physical Sciences at the Microscale, Department of Physics, University of Science and Technology of China, Hefei, Anhui 230026, China; [d]Department of Medical Sciences, Laboratory for Technologies of Advanced Therapies, University of Ferrara, Ferrara 44121, Italy; [e]NBS-C BioScience & Consulting GmbH, Vienna 1230, Austria; [f]Department of Chemistry, University of Hawaii, Honolulu, HI 96822; [g]Department of Cardiothoracic Surgery, New York University, New York, NY 10016; and [h]Department of Medicine, University of Montreal, Montreal, QC H1T 2M4, Canada

Edited by Bruce Beutler, The University of Texas Southwestern Medical Center, Dallas, TX, and approved October 25, 2021 (received for review June 28, 2021)

Carriers of heterozygous germline *BAP1* mutations (*BAP1*$^{+/-}$) are affected by the "BAP1 cancer syndrome." Although they can develop almost any cancer type, they are unusually susceptible to asbestos carcinogenesis and mesothelioma. Here we investigate why among all carcinogens, *BAP1* mutations cooperate with asbestos. Asbestos carcinogenesis and mesothelioma have been linked to a chronic inflammatory process promoted by the extracellular release of the high-mobility group box 1 protein (HMGB1). We report that *BAP1*$^{+/-}$ cells secrete increased amounts of HMGB1, and that *BAP1*$^{+/-}$ carriers have detectable serum levels of acetylated HMGB1 that further increase when they develop mesothelioma. We linked these findings to our discovery that BAP1 forms a trimeric protein complex with HMGB1 and with histone deacetylase 1 (HDAC1) that modulates HMGB1 acetylation and its release. Reduced BAP1 levels caused increased ubiquitylation and degradation of HDAC1, leading to increased acetylation of HMGB1 and its active secretion that in turn promoted mesothelial cell transformation.

mesothelioma | gene × environment | germline *BAP1* mutations | asbestos | HMGB1

Many—if not most—human cancers are a consequence of gene × environment interaction (G×E) (1, 2). G×E accounts for the observation that only a fraction of those exposed to environmental carcinogens develop cancer. Mesothelioma (3), for decades deemed as the example of a cancer caused almost exclusively by asbestos, has recently become a model to study G×E in cancer (1).

"Asbestos" identifies a family of six different carcinogenic mineral fibers whose use has been prohibited or strictly regulated since the 1980s (3). Only a fraction of asbestos workers developed mesothelioma: For example, about 4.6% of deaths among Caucasian South African asbestos miners were caused by mesothelioma (3, 4). Asbestos carcinogenesis has been linked to the release of HMGB1 by asbestos-exposed mesothelial cells and macrophages (3). HMGB1 is a ubiquitous nuclear protein that binds to chromatin and stabilizes nucleosomes, thus regulating transcription (5, 6). Under certain stress conditions, including asbestos exposure, HMGB1 translocates into the cytoplasm, where it regulates autophagy to prevent cell death (7, 8). Hypoacetylated HMGB1 localizes in the nucleus; instead, when HMGB1 is hyperacetylated, it is sequestered into the cytoplasm and from there it can be secreted (8–10). This process is regulated by histone deacetylases (HDACs), a family of enzymes that remove acetyl groups from histones and other nuclear proteins, including HMGB1 (11–13). Extracellular HMGB1 is a chemoattractant that promotes inflammation by recruiting macrophages, that in turn release mutagenic oxygen radicals, tumor necrosis factor alpha (TNFα), and other inflammatory cytokines (14). Mesothelial cells that die because of asbestos exposure passively release HMGB1, and those that survive asbestos exposure actively secrete HMGB1, promoting inflammation (14–18). Because asbestos remains in tissues for years, the inflammation becomes chronic and over time promotes mesothelioma development. Mesothelioma cells in turn secrete HMGB1 to promote their own growth (17, 19).

In addition to asbestos, mesothelioma is linked to germline heterozygous *BRCA1-associated protein 1* (*BAP1*) mutations: About one-third of carriers of inherited heterozygous *BAP1* mutations (*BAP1*$^{+/-}$) have developed mesothelioma, and two-thirds of sporadic mesotheliomas carry somatic biallelic *BAP1* mutations (20). Experiments in primary human mesothelial cells (HMs) with reduced BAP1 levels and in *Bap1*$^{+/-}$ mice

Significance

Our findings explain mechanistically the observed gene × environment (G×E) interaction in mesotheliomas occurring in carriers of heterozygous germline *BAP1* mutations (*BAP1*$^{+/-}$) exposed to asbestos. The increased amount of acetylated HMGB1 can be measured in the serum and may prove useful as a diagnostic/prognostic biomarker of mesothelioma in *BAP1*$^{+/-}$ individuals. Inhibition of HMGB1 secretion in *Bap1*$^{+/-}$ mutant mice exposed to asbestos significantly decreased the incidence of mesothelioma and prolonged the survival of those who developed mesothelioma. This strategy may be translated to carriers of germline *BAP1* mutations with the aim of decreasing their incidence of mesothelioma.

Author contributions: F.N., A.B., H.B., J.N.O., H.Y., and M.C. designed research; F.N., A.B., Q.W., F.B., S. Patergnani, J.S.S., F.K., E.H., M.T., H.B., C.G., and P.P. performed research; Q.W., F.B., F.K., R.X., Y.T., M.M., P.M., G.S., H.I.P., and J.N.O. contributed new reagents/analytic tools; F.N., A.B., Q.W., F.B., S. Patergnani, F.K., M.T., R.X., Y.T., M.M., S. Pastorino, H.B., G.G., C.G., P.P., J.N.O., H.Y., and M.C. analyzed data; and F.N., A.B., F.K., G.G., J.N.O., H.Y., and M.C. wrote the paper.

Competing interest statement: M.C. has a patent issued for BAP1. M.C. and H.Y. have two patents issued for HMGB1. M.C. is a board-certified pathologist who provides consultation for pleural pathology, including medical–legal.

This article is a PNAS Direct Submission.

[1]F.N. and A.B. contributed equally to this work.

[2]To whom correspondence may be addressed. Email: mcarbone@cc.hawaii.edu or haining@hawaii.edu.

This article contains supporting information online at http://www.pnas.org/lookup/suppl/doi:10.1073/pnas.2111946118/-/DCSupplemental.

Published November 23, 2021.

revealed that heterozygous *BAP1* mutations lower the threshold of asbestos exposure required to cause cellular transformation in vitro and mesothelioma in vivo, evidence of G×E (1). BAP1 is a ubiquitin carboxyl-terminal hydrolase (UCH), a member of the deubiquitylase family proteins. The strong tumor suppressor activity of BAP1 and its role in modulating G×E have been linked to its dual activity in the nucleus and in the cytoplasm (20). In the nucleus, where most BAP1 protein is detected, BAP1 has been implicated in DNA replication (21), repair (22), chromatin remodeling, and transcription (23, 24). In the cytoplasm, BAP1 regulates cell death (25–27) and mitochondrial metabolism (28). Cells with reduced or absent BAP1 activity are prone to malignant transformation as they accumulate DNA damage because they cannot efficiently repair the DNA (25). At the same time, their ability to execute apoptosis, ferroptosis, and possibly other forms of cell death is reduced (25–27, 29).

Since *BAP1* mutations increase susceptibility to asbestos, it appeared possible that the pathways regulated by BAP1 and HMGB1 might interact. Here we investigated the possible interplay between BAP1 and HMGB1, and we discovered that they bind to each other forming a trimeric complex with HDAC1. BAP1 deubiquitylated and stabilized HDAC1 allowing HDAC1 to deacetylate HMGB1, which is therefore retained in the nucleus. Reduced levels of BAP1 cause increased HDAC1 degradation and HMGB1 hyperacetylation, leading to extracellular release where HMGB1 promotes inflammation and mesothelial cell transformation.

Results

BAP1 Truncating Mutations Impair BAP1's Interaction with HMGB1. We discovered the "BAP1 cancer syndrome" (20) while studying families with high incidence of mesothelioma, including one from Louisiana (L family) and one from Wisconsin (W family) (30). $BAP1^{+/-}$ carriers have ~50% of wild-type (WT) BAP1 protein compared to unaffected family members (25). In $BAP1^{+/-}$ individuals from the L and W families, the respective mutated *BAP1* alleles code for truncated mutant proteins that lack the ability to localize to the nucleus (25).

Using proximity ligation assay (PLA) on fibroblast cell cultures from $BAP1^{+/-}$ carriers and age- and gender-matched wild-type *BAP1* ($BAP1^{WT}$) control family members (25), we detected that BAP1 and HMGB1 interact (Fig. 1*A*). We observed that the BAP1–HMGB1 interaction occurs predominantly in the cell nucleus, and that the number of discrete fluorescent PLA dots per cell was significantly lower in $BAP1^{+/-}$ fibroblasts compared to $BAP1^{WT}$ (Fig. 1*B*). This confirmed the specificity of the PLA signaling, because only the BAP1 protein encoded by the wild-type allele present in $BAP1^{+/-}$ cells can localize to the nucleus, resulting in a reduced amount of BAP1 bound to HMGB1 (25).

Coimmunoprecipitation (Co-IP) experiments confirmed that BAP1 interacts with HMGB1 and identified the BAP1 domain involved in the interaction (Fig. 1 *C* and *D*). We used HEK293 cells to overexpress Myc-tagged full-length BAP1, the catalytic inactive BAP1(C91S), the truncated BAP1(L) and BAP1(W) mutants, and deletion mutants encompassing the different BAP1 domains: N-terminal UCH domain, nonregular secondary structure (NORS) domain, C-terminal domain (CTD), and nuclear localization signal (NLS) domain (Fig. 1*C* and ref. 25). Cells were cotransfected with Flag-tagged HMGB1 and used as bait. We found that full-length BAP1 and the catalytic inactive BAP1(C91S) mutant coprecipitated with HMGB1, as detected by immunoblotting (Fig. 1*D*). Instead, the truncated mutants BAP1(L) and BAP1(W) did not interact with HMGB1. Accordingly, we discovered that the CTD-NLS of BAP1 is the domain that showed the strongest interaction with HMGB1 (Fig. 1*D*). In summary, we found that BAP1 and HMGB1 interact mostly in the nucleus, and that truncating mutations of BAP1 disrupt this interaction.

Reduced BAP1 Levels Increase HMGB1 Secretion. HMGB1 is the most abundant nonhistone nuclear protein, and, to some degree, it is also present in the cytoplasm, as it shuttles back and forth from the nucleus and accumulates into the cytosol prior to secretion (9, 31). We compared the subcellular localization of HMGB1 in $BAP1^{WT}$ and $BAP1^{+/-}$ primary human fibroblasts transfected with the nuclear marker H2B-RFP (Fig. 2*A*). Extranuclear HMGB1 was significantly ($P < 0.001$) increased in fibroblasts carrying germline $BAP1^{+/-}$ mutations, compared to $BAP1^{WT}$ (Fig. 2*B*). Conversely, nuclear HMGB1 levels were significantly ($P < 0.001$) lower in $BAP1^{+/-}$ compared to $BAP1^{WT}$ fibroblasts (Fig. 2*C*). Irrespective of the strong interaction, HMGB1 protein levels, mRNA levels, and half-life were not affected by BAP1 (*SI Appendix*, Fig. S1 *A–E*). Indeed, BAP1 did not deubiquitylate HMGB1 in vitro (*SI Appendix*, Fig. S1*F*).

We investigated whether the accumulation of HMGB1 in the cytoplasm of $BAP1^{+/-}$ fibroblasts resulted in HMGB1 secretion. HMGB1 levels were measured by enzyme-linked immunosorbent assay (ELISA) in conditioned cell culture media from $BAP1^{WT}$ and $BAP1^{+/-}$ primary human fibroblasts (Fig. 2*D*). We found higher HMGB1 levels in conditioned media from $BAP1^{+/-}$ fibroblasts; this finding was confirmed by immunoblot analysis (Fig. 2*E* and *SI Appendix*, Fig. S2 *A–C*). Downregulation of BAP1 protein levels with short interfering RNA (siRNA) also resulted in higher HMGB1 levels in conditioned media in $BAP1^{WT}$ fibroblasts (*SI Appendix*, Fig. S2*D*), in HM (Fig. 2*F*), and in THP-differentiated macrophages (Fig. 2*G*), compared to control cells (scramble siRNA).

We tested whether *BAP1* mutations could affect HMGB1 acetylation and subsequent extracellular release. Immunoprecipitation (IP) experiments of endogenous HMGB1 revealed higher levels of acetylated lysine residues in $BAP1^{+/-}$ fibroblasts, compared to $BAP1^{WT}$ (*SI Appendix*, Fig. S2*E*). Acetylation of key lysine residues within the two NLS sites of HMGB1 is known to promote active release of HMGB1 from activated monocytes and macrophages (9, 32), and possibly from other cell types. We explored whether HMGB1 acetylation at Lys12 (9, 33) could be responsible for the increased HMGB1 secretion we observed in $BAP1^{+/-}$ fibroblasts. By using a specific acetyl-Lys12 HMGB1 antibody, we found increased levels of acetyl-Lys12 HMGB1 in the conditioned media of $BAP1^{+/-}$ primary human fibroblasts compared to $BAP1^{WT}$ (Fig. 2*H*).

Mesothelioma cells grow out of a rich HMGB1 environment and they secrete HMGB1 sustaining their own growth in an autocrine fashion (17). Accordingly, HMGB1 can be measured in the conditioned media of mesothelioma cells and in the serum samples of mesothelioma patients and asbestos-exposed individuals (8, 14, 17, 19, 34). We detected higher levels of total and acetylated HMGB1 in the cell culture media of HP-3, a *BAP1* mutated mesothelioma cell line (35), compared to *BAP1* wild-type H2373 (*SI Appendix*, Fig. S2*F*). The higher levels of acetyl-HMGB1 in the HP-3 conditioned media were confirmed by ELISA (*SI Appendix*, Fig. S2*G*).

These results prompted us to test whether serum levels of HMGB1 and acetylated HMGB1 could be used as a biomarker to help discriminate $BAP1^{WT}$ and $BAP1^{+/-}$ family members and/or to reveal when $BAP1^{+/-}$ carriers developed mesothelioma. We tested by immunoblot the total serum levels of HMGB1 and of acetylated HMGB1 in $BAP1^{WT}$ individuals and $BAP1^{+/-}$ carriers from the L (Fig. 2*I*) and W (Fig. 2*J*) families. Moreover, serum HMGB1 was also tested in a $BAP1^{+/-}$ patient—a member of the W family—who had gone in remission after developing mesothelioma and whose serum we

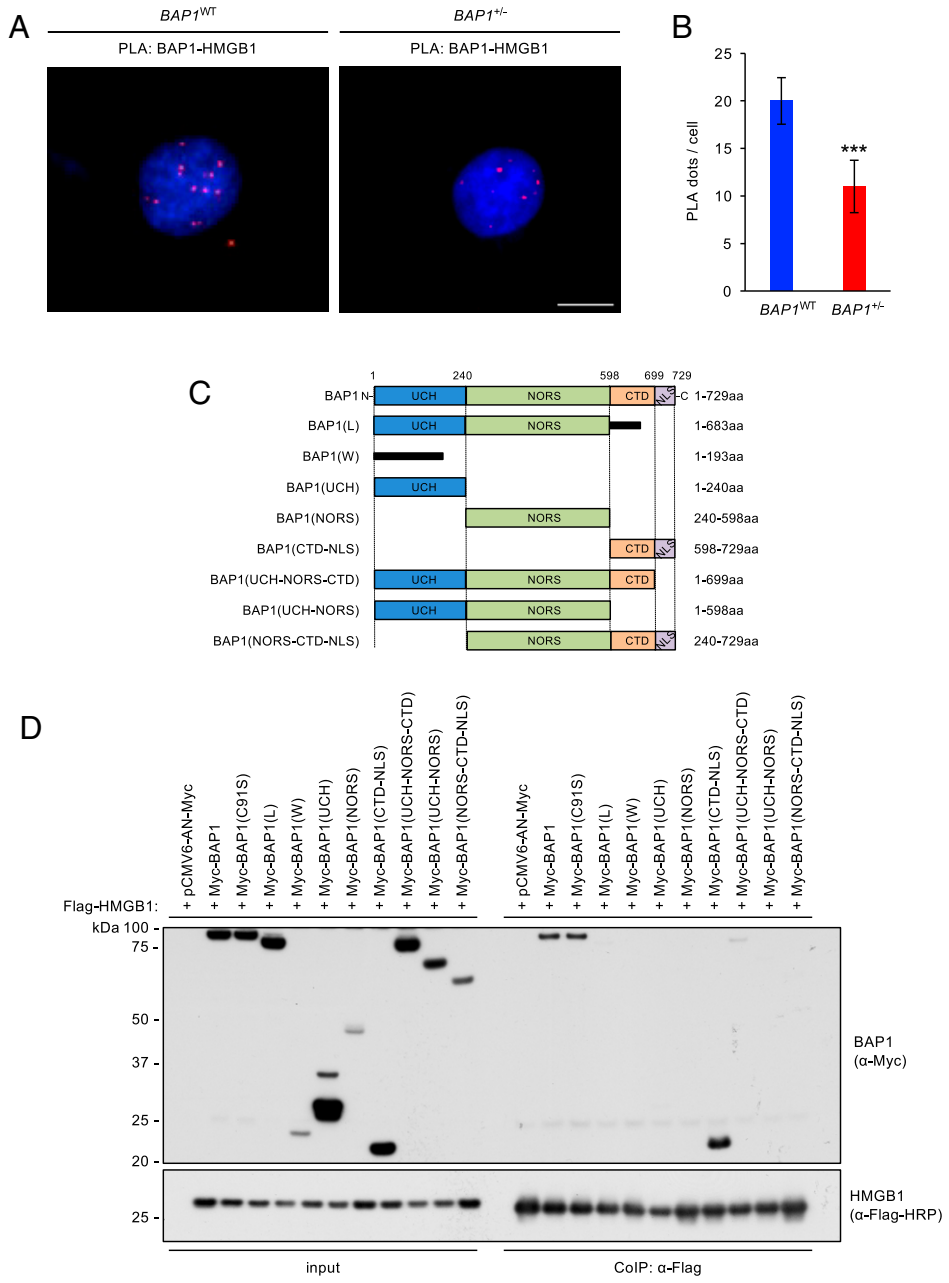

Fig. 1. BAP1 binds to HMGB1. (*A*) PLA showing the interaction of BAP1 and HMGB1 (red dots) in the nuclei of *BAP1*^{WT} and *BAP1*$^{+/-}$ fibroblasts (nuclei stained blue with DAPI); (Scale bar: 10 μM.) (*B*) Bar graph: Quantification of PLA red dots per cell showing reduced BAP1–HMGB1 interaction in *BAP1*$^{+/-}$ fibroblasts compared to *BAP1*^{WT}. Data shown are mean ± SD ($n = 6$ cells). *P* value was calculated using two-tailed unpaired Welch's *t* test, ***$P < 0.001$. (*C*) Schematic representation of full-length BAP1 (1 to 729 aa), the predicted truncations of BAP1 resulting from the germline mutations in the L (1 to 683 aa) and W (1 to 193 aa) families, and the different BAP1 domains: N-terminal ubiquitin carboxy (C)-terminal hydrolase (UCH) domain (aa 1 to 240), a NORS domain (aa 240 to 598), a CTD (aa 598 to 699), and a NLS (aa 699 to 729). Numbers refer to amino acid positions, see also ref. 25. (*D*) Co-IP: HEK293 cells were cotransfected with Flag-HMGB1 and the indicated Myc-tagged BAP1 expression vectors; cell extracts were used for Co-IP with anti-Flag resin. Both Myc-tagged BAP1 and its catalytically inactive isoform Myc-BAP1(C91S) interact with Flag-HMGB1, whereas the mutant constructs Myc-BAP1(L) and Myc-BAP1(W) lose the interaction with Flag-HMGB1. The BAP1 domain CTD-NLS had the highest binding affinity to Flag-HMGB1.

harvested while he was in remission and 10 y later when his mesothelioma relapsed (Fig. 2*J*). Serum levels of HMGB1 and acetylated HMGB1 were slightly higher in *BAP1*$^{+/-}$ carriers compared to *BAP1*^{WT}; however, a dramatic increase was observed in the *BAP1*$^{+/-}$ patient when his mesothelioma relapsed. Human specimens are limited, thus we sought to validate these findings in our *Bap1*$^{+/-}$ mouse model (36): We found that the serum levels of HMGB1 and acetylated HMGB1 increased upon asbestos exposure, and further drastically increased when *Bap1*$^{+/-}$ mice developed mesothelioma (Fig. 2*K*). In summary, we found that, reduced BAP1 levels resulted in increased HMGB1 acetylation and secretion in vitro and in vivo.

Higher Release of Acetylated HMGB1 in Cells Carrying *BAP1* Mutations Induces Malignant Transformation and Tumorigenesis. When HMs are exposed to asbestos in the presence of TNFα, a fraction of the cells undergo transformation and give rise to

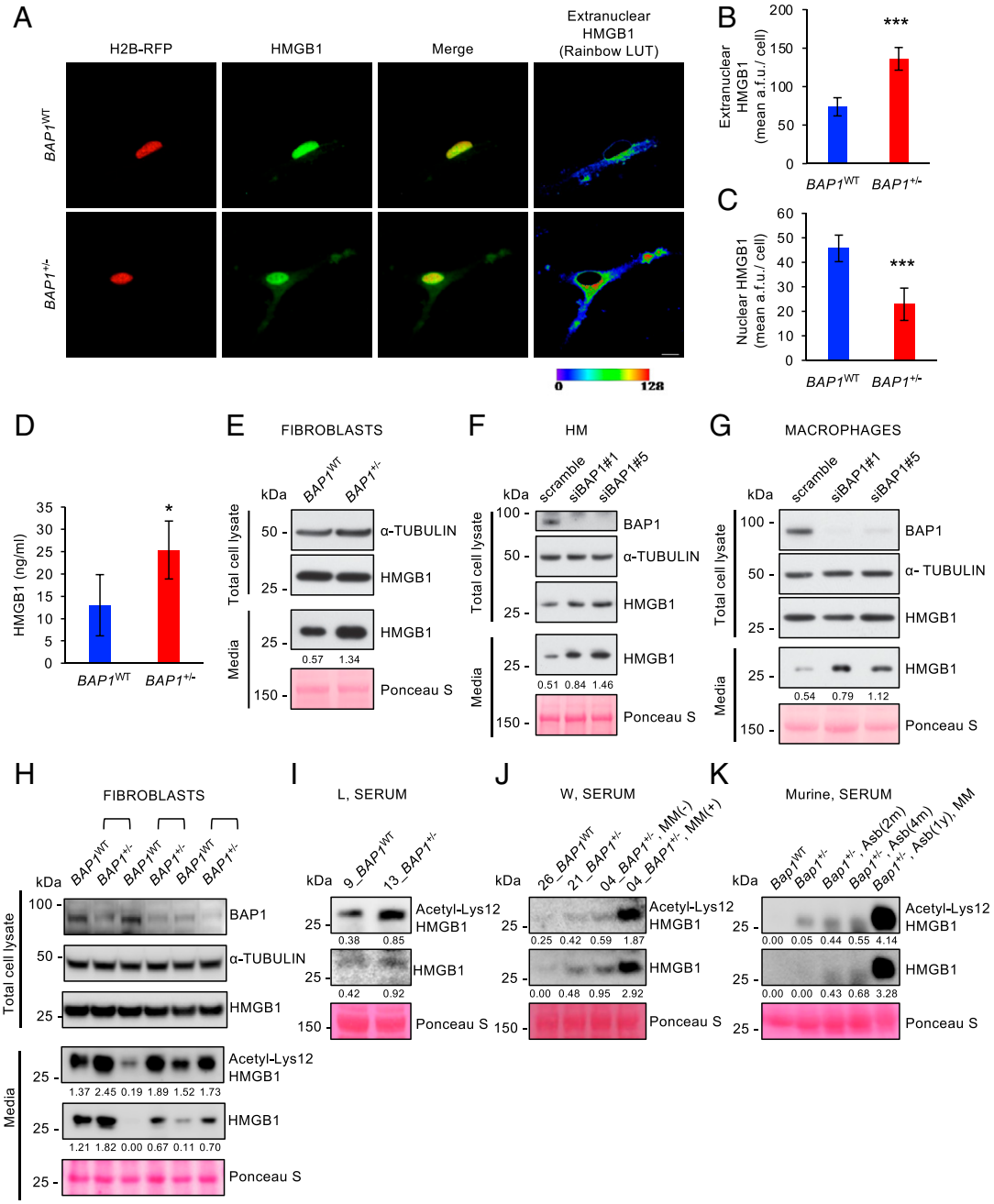

Fig. 2. Reduced BAP1 levels increase HMGB1 secretion. (*A*) Immunofluorescence: HMGB1 localization in *BAP1*^{WT} and *BAP1*$^{+/-}$ fibroblasts transfected with H2B-RFP (nuclear marker, red) and immune stained for HMGB1 (green). Merged images show the overlapping yellow signal between HMGB1 and H2B-RFP. The intensity of extranuclear HMGB1 was highlighted by adding a rainbow RGB (red, green, blue) LUT (lookup table) to the merged images. (Scale bar: 10 μM.) (*B* and *C*) Bar graphs: Quantification of extranuclear (*B*) and nuclear (*C*) HMGB1 measured as fluorescence intensity. Higher levels of extranuclear HMGB1 are seen in *BAP1*$^{+/-}$ fibroblasts, while higher levels of nuclear HMGB1 are seen in *BAP1*^{WT}fibroblasts. Data shown are mean ± SD (n = 10 cells per condition). (*D*) ELISA: Significantly higher HMGB1 levels in conditioned cell culture media of *BAP1*$^{+/-}$ fibroblasts compared to *BAP1*^{WT}; experiments were performed in technical duplicates, data shown are mean ± SD of n = 4 biological replicates of *BAP1*^{WT} and *BAP1*$^{+/-}$ fibroblasts matched by gender and age. (*E*) Immunoblot: Amounts of HMGB1 in the total cell lysate and in the conditioned cell culture media of *BAP1*^{WT} and *BAP1*$^{+/-}$ fibroblasts; increased HMGB1 levels were detected in the cell culture media of *BAP1*$^{+/-}$ fibroblasts compared to *BAP1*^{WT}. (*F* and *G*) Total cell lysate and conditioned media were analyzed by immunoblot in HMs (*F*) and in macrophages (*G*) transfected with control scramble siRNA, or siBAP1 (siBAP1#1 and siBAP1#5); *BAP1* silencing leads to an increased extracellular HMGB1 release in the conditioned media in all cellular models analyzed. (*H*) Total cell lysate and conditioned media were analyzed by immunoblot in different pairs of *BAP1*^{WT} and *BAP1*$^{+/-}$ fibroblasts from L family members; increased levels of actively secreted acetyl-Lys12 HMGB1 and HMGB1 were detected in the conditioned cell culture media of *BAP1*$^{+/-}$ compared to *BAP1*^{WT} fibroblasts. (*I* and *J*) Immunoblot of serum samples collected from L (*I*) and W family members (*J*). (*I*) Healthy L individuals matched by gender and age: 9_*BAP1*^{WT} and 13_*BAP1*$^{+/-}$. (*J*) Healthy W individuals matched by gender and age: 26_*BAP1*^{WT} and 21_*BAP1*$^{+/-}$, and one mesothelioma (MM) patient in remission 04_*BAP1*$^{+/-}$ MM(–) and when relapsed 10 y later, MM(+). Increased levels of acetyl-Lys12 HMGB1 and HMGB1 were present in sera of germline *BAP1*$^{+/-}$ mutation carriers, and an even greater increase was detected after mesothelioma relapsed. (*K*) Immunoblot of serum samples collected from healthy *Bap1*^{WT} and *Bap1*$^{+/-}$ mice, before and after (2 or 4 mo) asbestos injection, Asb(2m), Asb(4m), and 1 y after injection when the mouse developed MM [Asb(1y), MM]. Increased serum levels of acetyl-Lys12 HMGB1 were detected in the mouse carrying germline *Bap1*$^{+/-}$ mutations. Further increase was detected after asbestos exposure, and even more after MM developed. Decimals: *E–G*, HMGB1/Ponceau S; *H–K*, acetyl-Lys12 HMGB1/Ponceau S and HMGB1/Ponceau; *P* values were calculated using two-tailed unpaired Welch's *t* test, *$P < 0.05$, ***$P < 0.001$.

tridimensional foci. This in vitro assay has been used to assess carcinogenicity of mineral fibers (37, 38). Reduced BAP1 levels increase asbestos-induced HMs in vitro transformation, evidence of G×E interaction (25).

We tested whether the increased extracellular levels of total and acetylated HMGB1 in cells with reduced BAP1 levels (Fig. 2 and *SI Appendix*, Fig. S2) favor HM transformation. HMs transfected with siRNAs-BAP1 (siBAP1) and exposed to TNFα and crocidolite asbestos showed a significant increase in foci formation compared to controls (Fig. 3 *A–C*), supporting previous findings (25). Treatment with either BoxA, ethyl pyruvate (EP) or aspirin, drugs that inhibit HMGB1 (14, 17, 39–41), significantly reduced in vitro foci formation in BAP1-silenced HMs (Fig. 3 *A–C*). Aspirin decreased secretion of acetyl-Lys12 HMGB1 and HMGB1 in conditioned cell culture media of BAP1-silenced HMs (Fig. 3*D*). Thus, we investigated whether by inhibiting HMGB1 we could reduce the incidence of mesothelioma in mice carrying germline $Bap1^{+/-}$ mutations when exposed to asbestos. We used aspirin in these experiments, because 1) its primary metabolite, salicylic acid, binds and inhibits HMGB1 chemoattractant activity, an effect that contributes to the antiinflammatory activity of aspirin (41); and 2) aspirin is the only drug—among those listed above—that could conceivably be used in carriers of germline $BAP1^{+/-}$ mutations in a mesothelioma prevention trial.

We tested $Bap1^{+/-}$ mice divided into two groups of 75 mice each: Aspirin-treated and untreated, both injected with a total amount of 0.5 mg of crocidolite asbestos. The aspirin group consumed aspirin chow (400 ppm) throughout the duration of the study, a dose corresponding to ∼200 mg of aspirin per day in humans (*SI Appendix*). Ten weekly 0.05-mg intraperitoneal (i.p.) crocidolite injections began 1 wk after the aspirin treatment was initiated. Mice were monitored for 518 d after the last i.p. injection of crocidolite. The incidence of mesothelioma was significantly decreased in aspirin-treated $Bap1^{+/-}$ mice, $P = 0.0130$: In this group, 38% of the mice (25 of 65 mice) developed mesothelioma, compared with 62% (39 of 63 mice) in the untreated control group (Fig. 3*E*). Moreover, aspirin-treated $Bap1^{+/-}$ mice had a significantly higher mesothelioma-specific survival ($P = 0.0452$) compared to the untreated group (Fig. 3*F*).

BAP1 Deubiquitylates and Stabilizes HDAC1 Regulating Its Activity. In parallel, we investigated the mechanism by which BAP1 regulates HMGB1 secretion and tumorigenesis. Decreased nuclear activity of HDAC1 and HDAC4 promotes the hyperacetylation and subsequent release of HMGB1 (11–13). Because the levels of acetylated HMGB1 are increased in $BAP1^{+/-}$ fibroblasts, we used a fluorometric assay to assess nuclear HDAC activity in $BAP1^{WT}$ and $BAP1^{+/-}$ primary human fibroblasts. We found decreased nuclear HDAC activity in $BAP1^{+/-}$ fibroblasts compared to $BAP1^{WT}$ (Fig. 4*A* and *SI Appendix*, Fig. S3*A*). Total cell lysates from $BAP1^{+/-}$ fibroblasts contained reduced HDAC1 protein levels compared with $BAP1^{WT}$, while no differences were detected for HDAC4 levels (Fig. 4*B* and *SI Appendix*, Fig. S3*B*). HDAC1 and HDAC4 messenger RNA (mRNA) levels measured by qPCR with reverse transcription (qRT-PCR) were similar in $BAP1^{WT}$ and $BAP1^{+/-}$ fibroblasts (*SI Appendix*, Fig. S3*C*), indicating that the differences observed in HDAC1 levels were not transcriptionally regulated.

To test whether BAP1 modulates HMGB1 secretion through HDAC1 activity, we transduced $BAP1^{+/-}$ fibroblasts with an adenovirus encoding HDAC1. We found decreased secretion of acetyl-Lys12 HMGB1 and HMGB1 in the conditioned cell culture media of HDAC1-transduced $BAP1^{+/-}$ fibroblasts compared to control cells (Fig. 4*C*). We obtained similar results in HEK293 in which we overexpressed Flag-tagged HDAC1 (*SI Appendix*, Fig. S3*D*) and in HEK293 in which we silenced BAP1 and then overexpressed Flag-HDAC1 (*SI Appendix*, Fig. S3*E*).

Therefore, we tested the hypothesis that BAP1 might deubiquitylate and stabilize HDAC1. We transfected HEK293 cells with a Flag-tagged HDAC1, and Myc-tagged BAP1, BAP1(C91S), the truncated BAP1(L), and BAP1(W) mutants, or with the empty vector (pCMV6-AN-Myc) as control. A Flag resin was used as Co-IP bait, followed by in vitro ubiquitylation assay. We found that full-length BAP1, BAP1(C91S), as well as truncated BAP1(L) and BAP1(W) mutants, interacted with HDAC1 in vitro (Fig. 4*D*). Higher in vitro HDAC1 ubiquitylation was detected with the empty vector and with the catalytic inactive BAP1(C91S), indicating that BAP1 deubiquitylating activity was necessary to reduce HDAC1 ubiquitylation and to prevent its degradation (Fig. 4*D*). Mapping experiments (see also Fig. 1*C* and ref. 25) showed that the UCH domain of BAP1 alone can interact with HDAC1, explaining why the truncated mutants BAP1(L) and BAP1(W) retained the ability to interact and deubiquitylate HDAC1 in vitro (Fig. 4*E*). Nevertheless, the L and W mutants lack the NLS domain of BAP1; therefore in vivo they cannot translocate into the nucleus and deubiquitylate HDAC1. This explains why in total cell homogenates collected from primary human fibroblast cell cultures of $BAP1^{+/-}$ individuals, HDAC1 levels are reduced, and consequently HDAC enzymatic activity is lower than in cell homogenates from $BAP1^{WT}$ individuals.

HMGB1 Interacts with BAP1 and HDAC1. Since we demonstrated that BAP1 interacts with HMGB1 at its C-terminal CTD–NLS domain (598 to 729 amino acids [aa]) (Fig. 1*D*) and HDAC1 at its N-terminal UCH domain (1 to 240 aa) (Fig. 4*E*), we studied the reciprocal interactions among HMGB1, BAP1, and HDAC1. We found that HMGB1 coimmunoprecipitated both BAP1 and HDAC1 (Fig. 5*A*) in $BAP1^{WT}$ fibroblasts. In $BAP1^{+/-}$ fibroblasts, that have reduced amounts of both BAP1 and HDAC1 (Fig. 4*B* and *SI Appendix*, Fig. S3*B*), the amounts of BAP1 and HDAC1, coimmunoprecipitated with HMGB1, were reduced (Fig. 5*A*).

To test which domain of HMGB1 interacts with BAP1, HEK293 cells were cotransfected with Myc-tagged full-length BAP1 and full-length HMGB1 or HMGB1 deletion mutants encompassing the different protein domains (Fig. 5*B*). HMGB1 is a 25-kDa protein organized in three domains made up by two positively charged DNA-binding structures (A and B box) and a negatively charged acidic C tail (Fig. 5*B*). The deletion mutant spanning the entire A box and B box region (HMGB1-A/B box, 1 to 162 aa) displayed the strongest binding to BAP1 (Fig. 5*C*).

There is only one piece of published evidence (Co-IP assay) showing that HMGB1 binds to HDAC1 (42). We tested the HMGB1–HDAC1 interaction in HEK293 cells transfected with full-length HMGB1 or with the HMGB1 deletion mutants described in Fig. 4*B*. We found that endogenous HDAC1 strongly interacted with the HMGB1-A/B box domain (Fig. 5*D*). Our findings, in agreement with Xin et al. (42), validated the interaction of HDAC1 and HMGB1 supporting the hypothesis that HMGB1 is hyperacetylated when HDAC1 levels and activity are reduced.

HMGB1 (43), BAP1 (22), and HDAC1 (44) can bind the DNA directly or through recruitment by specific DNA-binding proteins. To test whether the interaction between BAP1, HMGB1, and HDAC1 was merely a consequence of their binding to the DNA, we performed Co-IP after complete degradation of the DNA with benzonase (an endonuclease that degrades all forms of DNA and RNA). We found that BAP1 bound both HMGB1 and HDAC1 even when the DNA was completely degraded (*SI Appendix*, Fig. S4 *A–D*).

BAP1 Stabilizes the Formation of a Trimeric Protein Complex with HMGB1 and HDAC1. BAP1, HMGB1, and HDAC1 coimmunoprecipitated, suggesting that they may form a trimer. To test

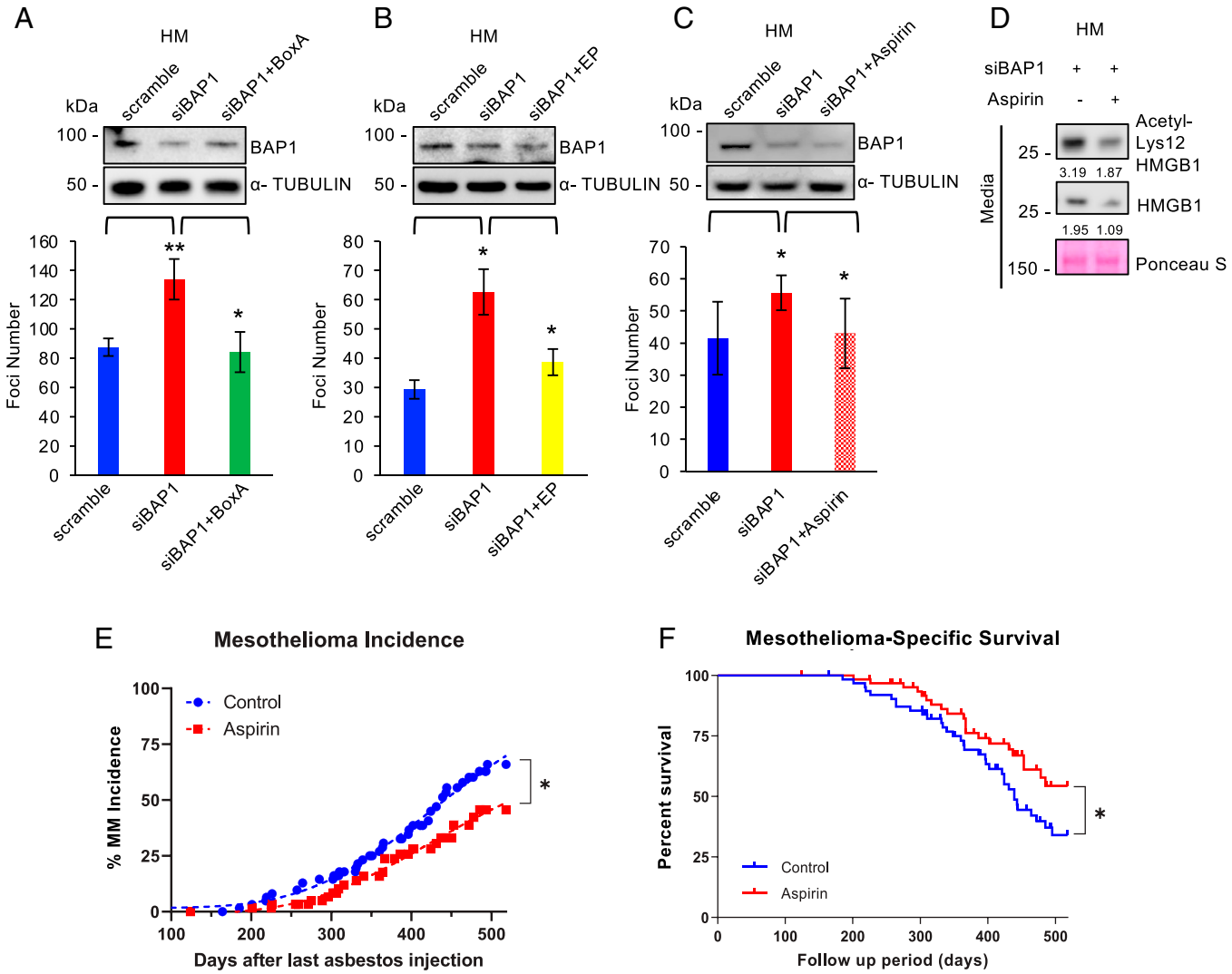

Fig. 3. BAP1 decreases HMGB1 secretion and malignant transformation. (*A*–*C*) In vitro transformation measured as tridimensional foci formation. Primary HM cells were silenced with scramble siRNA or a pool of siBAP1, and treated with 100 ng/mL Box A (*A*), or 10 mM EP (*B*), or 100 μM aspirin (*C*), and then exposed to crocidolite asbestos (5 μg/cm^2) in the presence of TNFα. Inhibition of HMGB1 secretion with Box A, EP, or aspirin, decreased foci formation in BAP1-silenced HMs. Data shown are mean ± SE of $n = 9$ technical replicates from $n = 3$ independent experiments (*A* and *B*), and of $n = 6$ technical replicates from $n = 2$ independent experiments (*C*). (*D*) Aspirin reduces the secretion of acetyl-Lys12 HMGB1 and HMGB1 in the conditioned cell culture media of HM cells transfected with a pool of siBAP1. Decimals: acetyl-Lys12 HMGB1/Ponceau S, HMGB1/Ponceau S. (*E* and *F*) Mesothelioma incidence (*E*) and mesothelioma-specific survival (*F*) in aspirin-treated *Bap1*$^{+/-}$ mice after exposure to crocidolite. For mesothelioma incidence, *P* value was calculated using Fisher's exact test ($P = 0.0130$); survival curves were compared using Log-rank test ($P = 0.0452$). *P* values were calculated using two-tailed unpaired Welch's *t* test, $^{**}P < 0.01$, $^{*}P < 0.05$. We had to exclude 12 and 10 mice from each group, respectively, from analysis because the cause of death was due to factors unrelated to asbestos exposure.

this hypothesis, we performed surface plasmon resonance (SPR) using recombinantly expressed human proteins. In a sequential injection experiment, we tested the binding of HDAC1, followed by BAP1, to HMGB1, immobilized as a ligand on the surface of an optical sensor chip (Fig. 6*A*). The resulting sensorgram indicates the ability of the analyte proteins HDAC1 and BAP1 to simultaneously form binding complexes on the ligand HMGB1 (Fig. 6*A*). We performed a kinetic binding analysis to assess the strength of the interactions of BAP1–HMGB1 and BAP1–HDAC1, in comparison to the interaction of HMGB1–HDAC1. Recombinant BAP1 and HDAC1 were passed over the immobilized ligands, HMGB1 or BAP1, at four concentrations in single binding cycles. Buffer subtracted sensorgram overlays were generated and used for kinetic binding analysis. Kinetic binding constants were determined by mathematical sensorgram fitting (*Materials and Methods*). Single analyte binding kinetics indicate that BAP1 interacts independently and strongly with HMGB1 (Fig. 6*B*) and HDAC1 (Fig. 6*C*) with 3.8 ± 1.5 nM (*SI Appendix*, Fig. S5*A*) and 17.1 ± 7.7 nM (*SI Appendix*, Fig. S5*B*) affinity, respectively. HMGB1 also interacted independently with HDAC1 (Fig. 6*D*), with 24.1 ± 14.4 nM affinity (*SI Appendix*, Fig. S5*C*). Therefore, the affinity of BAP1 for HMGB1 and HDAC1 is higher than the affinity of HDAC1 for HMGB1. These higher BAP1 affinities are caused by faster on-rates. We further analyzed the binding kinetic of a BAP1–HDAC1 complex to immobilized HMGB1 (Fig. 6*E*), discovering that a preformed complex was able to bind to the HMGB1 ligand. Sensorgram fitting revealed that the preformed BAP1–HDAC1 complex binds to HMGB1 with 1.2 ± 0.7 nM affinity (*SI Appendix*, Fig. S5*D*), which is higher than the affinity measured for the binding of free HDAC1 to HMGB1 ($K_D = 24$.

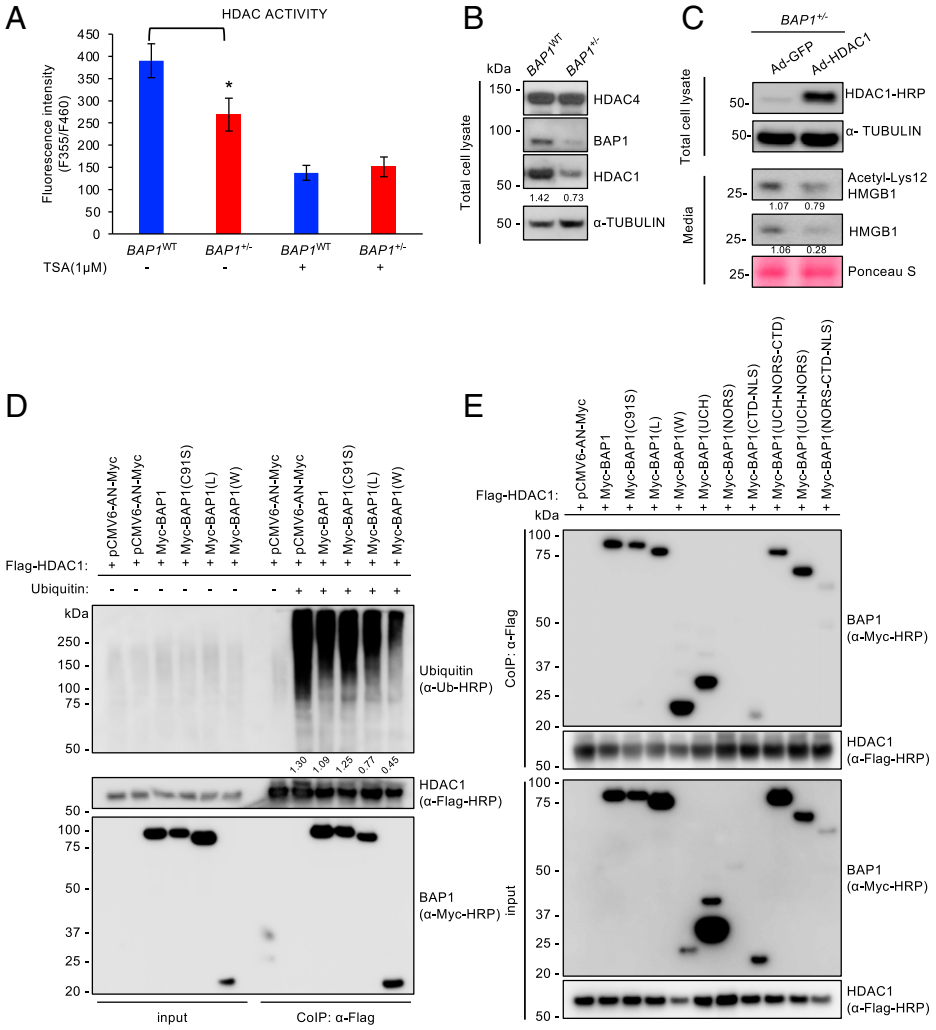

Fig. 4. BAP1 prevents HDAC1 degradation. (*A*) Fluorimetric assay. Reduced HDAC activity in fibroblasts carrying germline *BAP1*$^{+/-}$ mutations. Data of in vitro HDAC activity assay on nuclear extracts are displayed as mean ± SE of $n = 7$ biological replicates of *BAP1*^{WT} and *BAP1*$^{+/-}$ fibroblasts matched by gender and age ($n = 4$ from W and $n = 3$ from L family members). Trichostatin A (TSA), a HDAC inhibitor, was utilized to check the specificity of the HDAC activity assay. *P* value was calculated using two-tailed unpaired Welch's *t* test, *$P < 0.05$. (*B*) Immunoblot of HDAC1 and HDAC4 protein levels in total cell lysates of *BAP1*^{WT} and *BAP1*$^{+/-}$ fibroblasts showing reduced HDAC1 in *BAP1*$^{+/-}$ compared to *BAP1*^{WT} fibroblasts. Decimals: HDAC1/α-tubulin. (*C*) Immunoblot: Reintroduction of HDAC1 decreases the secretion of HMGB1 and acetyl-Lys12 HMGB1 in the conditioned cell culture media of *BAP1*$^{+/-}$ fibroblasts compared to control cells. Decimals: Acetyl-Lys12 HMGB1/Ponceau S and HMGB1/Ponceau S. (*D*) In vitro ubiquitylation assay. HEK293 cells were cotransfected with Flag-tagged HDAC1 and Myc-tagged wild-type BAP1, the catalytically inactive BAP1(C91S), BAP1(L) and BAP1(W), pCMV6-AN-Myc was used as a negative control. Wild-type BAP1 interacts and deubiquitylates HDAC1 compared to BAP1(C91S); truncated BAP1(L) and BAP1(W) are also able to interact and deubiquitylate HDAC1 in vitro. Decimals: Ubiquitin/HDAC1. (*E*) Mapping of the BAP1 region interacting with HDAC1. HEK293 cells were cotransfected with Flag-HDAC1 and the indicated Myc-tagged BAP1 expression vectors (see also Fig. 1*C*); cell extracts were used for Co-IP with anti-Flag resin. The UCH domain of BAP1 had the highest binding affinity to HDAC1, while the NORS region alone showed no interaction, and the CTD-NLS region only slightly contributed to the binding.

1 ± 14.4 nM). Therefore, the presence of BAP1 in a protein complex with HDAC1 and HMGB1 stabilizes this trimer, resulting in a lower complex dissociation rate (*SI Appendix*, Fig. S5*D*).

Fig. 6*F* shows the computational structural model of the BAP1–HMGB1–HDAC1 binding complex. BAP1 appears as a bent structure due to the interdomain interactions between its N terminus (the UCH domain, Fig. 6*F*, blue) and the C terminus (the CTD domain, Fig. 6*F*, yellow). The NORS domain (Fig. 6*F*, pink) in the middle is highly disordered. Here we present a possible conformation of the NORS domain connecting to the N and C terminus of BAP1. However, the NORS domain has a large variety of conformations, and the NLS domain of BAP1 is also highly disordered (*SI Appendix*, Fig. S6*A*). Our ab initio physical simulations predict that HMGB1 (Fig. 6*F*, red) utilizes its A box and B box to wrap around the central helix of the CTD domain of BAP1 (ranging from residue 670 to 700). Both the A box and B box of HMGB1 make contacts with BAP1, thus contributing to the overall stability of the binding complex. This prediction is consistent with our finding that deleting either the A box or the B box of HMGB1 decreases the binding affinity of HMGB1 to BAP1 (Fig. 5*C*). Our structural model indicates that the binding between HMGB1 and BAP1 is largely mediated by hydrophobic interactions. In the WT model (Fig. 6*F*), the B box of HMGB1 (residues 102F and 103F) and BAP1 (residues 675I, 678F, and 682L) form a critical hydrophobic patch. The binding mode between HMGB1 and BAP1 changed when these five residues were mutated to alanine (*SI Appendix*, Fig. S6 *B–D*). The interaction between the two proteins, however, was weakened but not abolished (*SI Appendix*, Fig. S6 *B–D*). Docking of HDAC1

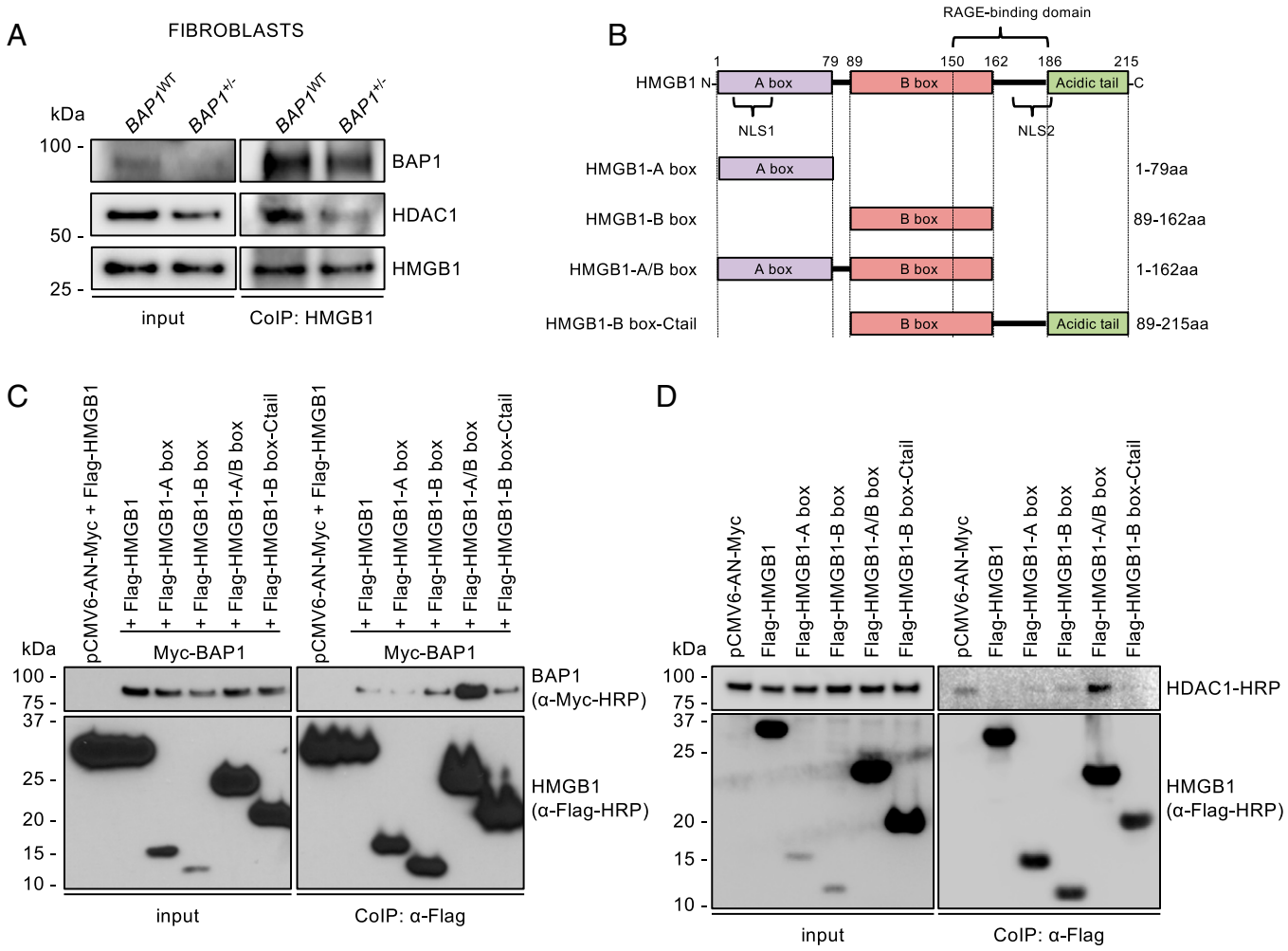

Fig. 5. Characterization of HMGB1 binding to BAP1 and HDAC1. (*A*) Co-IP of endogenous BAP1 and HDAC1 with HMGB1 (used as bait) in fibroblast cell cultures from *BAP1*^{WT} individuals or carriers of heterozygous *BAP1*$^{+/-}$ mutations. Higher amounts of the coprecipitated BAP1–HDAC1 proteins are found in *BAP1*^{WT} cells. (*B*) Schematic representation of HMGB1 domains. HMGB1 (1 to 215 amino acids) consists of an N-terminal A box domain (aa 1 to 79), a B box domain (aa 89 to 162), and a C-terminal acidic tail (aa 186 to 215). Numbers refer to amino acid (aa) positions. (*C*) Mapping of the HMGB1 region interacting with BAP1. HEK293 cells were cotransfected with Myc-tagged BAP1 and the Flag-tagged HMGB1 fragments displayed in *B*. Cell extracts were used for Co-IP with anti-Flag resin. The HMGB1-A/B box domain had the strongest binding affinity to Myc-tagged BAP1; A box and B box domains alone showed weaker interaction, and the B box-Ctail region slightly contributed to the binding. (*D*) Mapping of the HMGB1 region interacting with HDAC1. HEK293 cells were cotransfected with the indicated Flag-tagged HMGB1 fragments (*B*). Cell extracts were used for Co-IP with an anti-Flag resin. The HMGB1-A/B box domain showed the strongest binding affinity to endogenous HDAC1.

to the BAP1–HMGB1 complex resulted in the simultaneous interaction of HDAC1 (Fig. 6*F*, gray) with BAP1 and HMGB1. This computational analysis supports the experimental findings that BAP1–HMGB1–HDAC1 forms a trimeric protein complex and provides a structural model of the trimer.

Discussion

BAP1 regulates G×E interaction in human cancer (1). Previous studies revealed that impaired DNA repair by homologous recombination in carriers of *BAP1*$^{+/-}$ mutations favors the accumulation of genetic damage upon exposure to asbestos. DNA damaged cells are eliminated by apoptosis, a process that is significantly reduced in *BAP1*$^{+/-}$ mutation carriers because BAP1 prevents the degradation of Ca^{2+} channels in the endoplasmic reticulum (ER), which release Ca^{2+} from the ER to the mitochondria, where Ca^{2+} regulates cell death (25). Mitochondrial metabolism is also affected, favoring aerobic glycolysis (28). These activities account for the potent tumor suppressor activity of BAP1 but do not explain the preferential G×E interaction with asbestos. For example, *TP53* is also a potent tumor suppressor that similarly to BAP1 simultaneously regulates DNA repair by homologous recombination, apoptosis, and mitochondrial metabolism. Heterozygous germline mutations of *BAP1* cause the BAP1 cancer syndrome, while *TP53* mutations cause Li–Fraumeni syndrome, both characterized by high cancer penetrance: ∼100% of affected individuals develop one or more cancers during their lifetime (1). The tumor spectrum, however, is quite different: Germline *BAP1* mutations cooperate with asbestos and preferentially cause mesothelioma, while germline *TP53* mutations interact with ionizing radiations and smoke, not with asbestos, in causing cancer in humans (1, 20). Thus, one of the main puzzles that we have faced studying the role of *BAP1* in cancer is to understand why *BAP1* preferentially acts in concert with asbestos to cause mesothelioma rather than with other carcinogens.

The findings we present provide a mechanistic rationale for the G×E between *BAP1* mutations, asbestos-induced chronic inflammation, and mesothelioma (Fig. 7). We discovered that BAP1 simultaneously binds to HMGB1 and HDAC1, and that

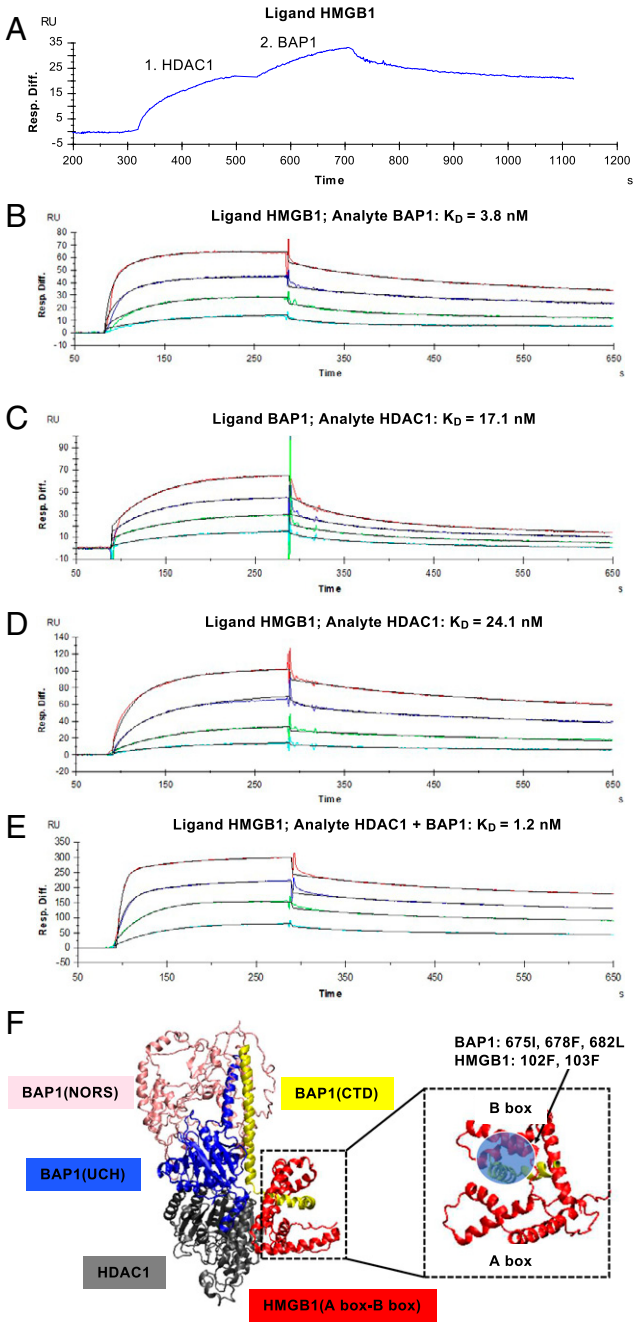

Fig. 6. BAP1, HDAC1, and HMGB1 form a trimeric protein complex. (*A*) SPR sensorgram showing analyte binding of HDAC1 and BAP1 (167 nM), sequentially passed over immobilized HMGB1 without intermediate chip surface regeneration. (*B–D*) Sensorgrams and fitted curves, applying a Langmuir 1:1 binding model. Analytes were bound in serial dilutions (red: 167 nM, blue: 84 nM, green: 42 nM, turquoise: 21 nM) to the ligand covalently immobilized on the surface of a Biacore CM5 sensor chip. Binding of BAP1 to HMGB1 (*B*); binding of HDAC1 to BAP1 (*C*); binding of HDAC1 to HMGB1 (*D*). (*E*) HDAC1 and BAP1 were coincubated in serial dilutions (red: 167 nM, blue: 84 nM, green: 42 nM, turquoise: 21 nM) for 10 min in HBS-EP buffer. The preformed complexes were subsequently passed as analyte over the immobilized HMGB1 ligand. Kinetic constants and affinity were determined from the concentration sensorgrams by Langmuir 1:1 curve fitting. The equilibrium dissociation constants (K_D; in nanomoles) are shown. (*F*) Structural model of the BAP1–HMGB1–HDAC1 trimeric protein complex. BAP1: UCH, blue; NORS, pink; CTD, yellow; HMGB1 (A box–B box), red; HDAC1, gray. The binding interface between BAP1 and HMGB1 is zoomed in. The hydrophobic patch between the B box of HMGB1 and BAP1 is highlighted: light blue circle.

BAP1 stabilizes the formation of this trimeric protein complex. In this trimeric protein complex, BAP1 does not deubiquitylate HMGB1; instead BAP1 deubiquitylates and stabilizes HDAC1, allowing HDAC1 to deacetylate HMGB1, which is therefore retained in the nucleus where HMGB1 increases nucleosomal occupancy (i.e., the fraction of DNA assembled into nucleosomes) (45). We found that reduced levels of BAP1 in carriers of germline *BAP1* mutations increased HDAC1 ubiquitylation and degradation, which in turn caused increased acetylated HMGB1 that is released into the extracellular milieu where HMGB1 promotes inflammation and mesothelial cell transformation (Fig. 7). Secretion of HMGB1 reduced nuclear HMGB1 levels (Fig. 2 *A–C*), which in turn reduces nucleosome assembly (45), exposing the DNA to damage caused by reactive oxygen species produced at sites of asbestos deposition (19). These findings may also be relevant to other malignancies that develop in carriers of germline *BAP1* mutations.

Treatment with the HMGB1 inhibitors BoxA, EP, and aspirin significantly reduced the in vitro transformation of asbestos-exposed HMs in which BAP1 was silenced. We linked these effects to the reduced levels of secreted acetylated HMGB1 observed upon aspirin treatment, supporting previous data showing that aspirin binds and inhibits HMGB1 chemoattractant activity (41, 46). Aspirin therapy significantly reduced the incidence of mesothelioma in *Bap1*$^{+/-}$ mutant mice exposed to asbestos and increased the survival of those mice that developed mesothelioma. However, aspirin has also additional antiinflammatory activities that may contribute to these results. Regardless, our findings are relevant to *BAP1*$^{+/-}$ carriers who are very susceptible to asbestos carcinogenesis and mesothelioma (3, 47).

Over 60% of mesotheliomas contain tumor cells with biallelic somatic *BAP1* inactivating mutations (48, 49). Our results indicate that these tumors because of reduced HDAC1 activity may secrete higher amounts of HMGB1 in the microenvironment facilitating tumor growth (17). Therefore, our findings may help explain why in the VANTAGE 014 study (vorinostat in patients with advanced malignant pleural mesothelioma who have progressed on previous chemotherapy), a phase 3 trial including

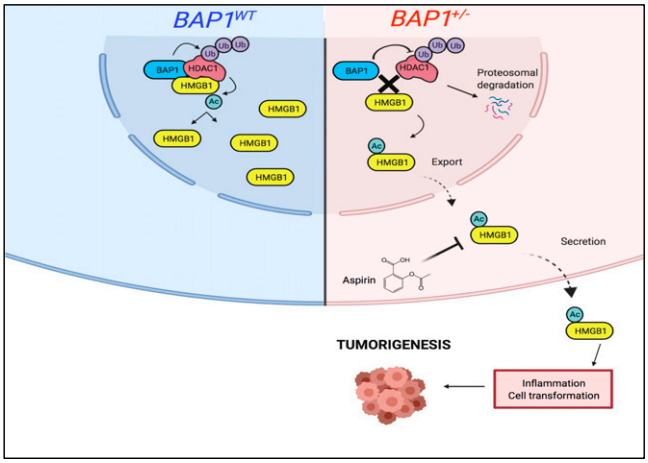

Fig. 7. BAP1, HDAC1, and HMGB1 trimer regulates chronic inflammation and cell transformation. Schematic representation showing how BAP1 prevents active HMGB1 release through the stabilization of HDAC1. In *BAP1*^{WT} individuals, nuclear BAP1 forms a trimer with HMGB1 and HDAC1. BAP1 deubiquitylates and stabilizes HDAC1, which can deacetylate HMGB1, thus preventing its active secretion. In *BAP1*$^{+/-}$ carriers, reduced BAP1 levels result in the degradation of HDAC1 and destabilization of its binding to HMGB1, leading to increased acetylation of HMGB1. Acetylated HMGB1 is then secreted into the extracellular space and promotes chronic inflammation and cell transformation, contributing to the development of mesothelioma. Aspirin by blocking HMGB1 secretion inhibits mesothelial cell transformation and tumorigenesis. Image was made with BioRender.com.

661 patients, the HDAC inhibitor vorinostat did not improve overall survival in an unselected group of mesothelioma patients compared with those treated with standard of care (50).

In the past decades, cancer researchers focused largely at identifying human carcinogens to reduce exposure (51). The recent realization that most cancers occur in a contest of G×E interaction in which exposure to certain carcinogens is more harmful to some than others based on an individual's genetics, has led to the new developing field of personalized cancer prevention and therapy. Germline testing allows for the identification of carriers of germline mutations of tumor suppressor genes affected by various cancer syndromes. These individuals are very susceptible to developing cancer, especially upon exposure to carcinogens (1). Some of the carcinogens involved have been identified: Among them, asbestos acts in concert with germline heterozygous *BAP1*$^{+/-}$ mutations to cause mesothelioma; chronic inflammation promotes colon cancer in individuals affected by Lynch syndrome (LS), etc. (1). By elucidating the mechanisms underlying these different G×E interactions, it is possible to target these mechanisms for cancer prevention, early detection, and therapy. For example, the discovery that TSC1 and TSC2 inhibit mTORC1 led to the treatment of tumors developing in patients affected by tuberous sclerosis with the mTORC inhibitor rapamycin (sirolimus) (52). Similarly, we hope that our discovery of the mechanism that underlies G×E in carriers of germline *BAP1*$^{+/-}$ mutations exposed to asbestos may lead to novel therapies. Our findings in mice suggest that *BAP1*$^{+/-}$ germline mutation carriers may benefit from daily aspirin treatment as observed, for example, in those individuals affected by Lynch syndrome in which daily aspirin therapy significantly decreased the incidence of colon cancer. Moreover, although mesothelioma is one of the most well-characterized HMGB1-related tumor models (14, 17, 34), the relevance of extracellular HMGB1 to carcinogenesis has also been proposed in other inflammation-related malignancies (53–56). The increased amount of acetylated HMGB1 can be measured in the serum and may prove useful to monitor carriers of *BAP1*$^{+/-}$ mutations for early detection of mesothelioma and possibly of other cancers, and/or for recurrence after surgical resection, something we are testing in an ongoing biomarker study sponsored by the Early Detection Research Network of the National Cancer Institute.

In conclusion, our findings provide a mechanistic rationale for G×E among *BAP1* mutations, asbestos-induced chronic inflammation, and carcinogenesis. By interfering with these mechanisms, we reduced the incidence of mesothelioma in mice carrying germline *Bap1*$^{+/-}$ mutations exposed to asbestos; a similar strategy may be effective in individuals carrying germline *BAP1*$^{+/-}$ mutations.

Materials and Methods

Subjects. The collection and use of patient information and samples were approved by the Institutional Review Board (IRB) of the University of Hawaii (IRB no. CHS14406). Participants were referred to the study by collaborators or by word of mouth. Adequate time was provided to participants to go over study information along with information regarding risks, benefits, and alternative options. It was explained that the study is for research purposes only and they are allowed to withdraw their consent at any time. Each participant who consented was also given a coded number to protect his or her information.

Cell Cultures and Animal Studies. Human dermal skin fibroblasts from explants of skin biopsies were collected, as previously described (25).

The 9- to 15-wk-old *Bap1*$^{+/-}$ mice (36) were divided into two groups of 75 (37 males and 38 females) mice each: Aspirin treated and untreated. Aspirin treatments were administered with 400 ppm aspirin chow (custom standard irradiated chow, Envigo) ad libitum throughout the duration of the study. The control group received standard chow (Envigo). Ten weekly 0.05-mg i.p. crocidolite injections began 1 wk after aspirin treatment. Mice were monitored for a 518-d follow-up period after the last i.p. injection of crocidolite asbestos. Mice were handled in accordance with the University of Hawaii Institutional Animal Care and Use Committee (Protocol 06-032) guidelines.

Reagents. Crocidolite asbestos fibers were obtained from SPI-Chem (02704A-AB) and processed as previously described (14, 57). Average length and diameter of reference crocidolite fibers were 3.2 ± 1 μm and 0.22 ± 0.01 μm, respectively. BoxA, the lipopolysaccharide (LPS)-free HMGB1 truncated form, was obtained from HMG Biotech. EP was obtained from Sigma-Aldrich (E47808). Benzonase was from Sigma-Aldrich (E1014-5KU). Aspirin was from Sigma-Aldrich (A5376). siRNA oligonucleotides were obtained from Qiagen. Expression plasmids were generated by Blue Heron Biotech. Adenoviruses expressing HDAC1 and GFP were purchased from SignaGen Laboratories (Ad-HDAC1, catalog no. SL101010; Ad-GFP, catalog no. SL100708).

Technical Procedures. Immunoblotting, qPCR, in vitro HDAC assay, Co-IP, in vitro ubiquitylation assay, immunofluorescence, Duolink proximity ligation in situ assay, and in vitro cell transformation assay, were performed according to standard techniques and as described in ref. 25.

Analysis of Total and Acetylated HMGB1 Levels in Conditioned Cell Culture Media. The levels of total and acetylated HMGB1 were detected with anti-HMGB1 (Abcam, ab79823), and anti–acetyl-Lys12(AC-K12)-HMG-1 (Signalway Antibody, SAB, cat. no. HW144) antibodies, respectively.

The amount of acetylated HMGB1 released in the conditioned media of fibroblasts and mesothelioma cells was also analyzed by ELISA, using the human HMGB1 ELISA kit with modifications (IBL International, cat. no. ST51011).

Computational Modeling of the BAP1–HMGB1–HDAC1 Complex. See refs. 58–60 and *SI Appendix*.

SPR Experiments. See *SI Appendix*.

Data Availability. All study data are included in the article and/or supporting information.

ACKNOWLEDGMENTS. We are grateful to the members of the Louisiana and Wisconsin families who donated their specimens to our research. We thank our college student Abigail Sipes for helping us prepare the figures, Christine Ruf from NBS-C BioScience & Consulting GmbH for assistance with the SPR, Dr. Affar El Bachir for providing support for H.B., and Drs. Anwesha Dey and Vishva M. Dixit at the Department of Discovery Oncology, Genentech, South San Francisco CA for creating and providing the *Bap1* mutant mouse model. Funding was provided by the National Institute of Environmental Health Sciences 1R01ES030948-01 (M.C. and H.Y.), the National Cancer Institute (NCI) 1R01CA237235-01A1 (M.C. and H.Y.) and 1R01CA198138 (M.C.), the Department of Defense W81XWH-16-1-0440 (H.Y., M.C., and H.I.P.), and from the University of Hawaii Foundation through donations from: the Riviera United-4-a Cure (M.C. and H.Y.), the Melohn Family Endowment, Honeywell International Inc., the Germaine Hope Brennan Foundation, and the Maurice and Joanna Sullivan Family Foundation (M.C.). H.I.P. and H.Y. report funding from the Early Detection Research Network NCI 5U01CA214195-04. H.I.P. reports funding from Genentech, Belluck and Fox LLP. The work of Q.W., J.N.O., F.B., and Q.W. was supported by the NSF (Grants PHY-2019745 and CHE-1614101) and by the Welch Foundation (Grant C-1792). P.P. and C.G. report funding from the Italian Association for Cancer Research (IG-23670 to P.P. and IG-19803 to C.G.), AROSE, Progetti di Rilevante Interesse Nazionale (PRIN2017E5L5P3 to P.P. and PRIN20177E9EPY to C.G.), the Italian Ministry of Health (GR-2013-02356747 to C.G.), the European Research Council (853057-InflaPML to C.G.), and local funds from the University of Ferrara. S. Patergnani was supported by "Fondazione Umberto Veronesi." Work at the the Center for Theoretical Biological Physics was supported by the NSF (Grant PHY-2019745). Additional support was provided by NSF Grant CHE-1614101. J.N.O. is a Cancer Prevention and Research Institute of Texas Scholar in Cancer Research.

1. M. Carbone *et al.*, Tumour predisposition and cancer syndromes as models to study gene-environment interactions. *Nat. Rev. Cancer* **20**, 533–549 10.1038/s41568-020-0265-y. (2020).
2. M. Carbone *et al.*, Consensus report of the 8 and 9th Weinman Symposia on Gene x Environment Interaction in carcinogenesis: Novel opportunities for precision medicine. *Cell Death Differ.* **25**, 1885–1904 (2018).
3. M. Carbone *et al.*, Mesothelioma: Scientific clues for prevention, diagnosis, and therapy. *CA Cancer J. Clin.* **69**, 402–429 (2019).
4. G. K. Sluis-Cremer, F. D. Liddell, W. P. Logan, B. N. Bezuidenhout, The mortality of amphibole miners in South Africa, 1946-80. *Br. J. Ind. Med.* **49**, 566–575 (1992).

5. M. E. Bianchi *et al.*, High-mobility group box 1 protein orchestrates responses to tissue damage via inflammation, innate and adaptive immunity, and tissue repair. *Immunol. Rev.* **280**, 74–82 (2017).
6. M. T. Lotze, K. J. Tracey, High-mobility group box 1 protein (HMGB1): Nuclear weapon in the immune arsenal. *Nat. Rev. Immunol.* **5**, 331–342 (2005).
7. D. Tang *et al.*, Endogenous HMGB1 regulates autophagy. *J. Cell Biol.* **190**, 881–892 (2010).
8. J. Xue *et al.*, Asbestos induces mesothelial cell transformation via HMGB1-driven autophagy. *Proc. Natl. Acad. Sci. U.S.A.* **117**, 25543–25552 (2020).
9. T. Bonaldi *et al.*, Monocytic cells hyperacetylate chromatin protein HMGB1 to redirect it towards secretion. *EMBO J.* **22**, 5551–5560 (2003).
10. B. Lu *et al.*, JAK/STAT1 signaling promotes HMGB1 hyperacetylation and nuclear translocation. *Proc. Natl. Acad. Sci. U.S.A.* **111**, 3068–3073 (2014).
11. J. Evankovich *et al.*, High mobility group box 1 release from hepatocytes during ischemia and reperfusion injury is mediated by decreased histone deacetylase activity. *J. Biol. Chem.* **285**, 39888–39897 (2010).
12. J. Y. Zou, F. T. Crews, Release of neuronal HMGB1 by ethanol through decreased HDAC activity activates brain neuroimmune signaling. *PLoS One* **9**, e87915 (2014).
13. S. Fu *et al.*, Crosstalk between hepatitis B virus X and high-mobility group box 1 facilitates autophagy in hepatocytes. *Mol. Oncol.* **12**, 322–338 (2018).
14. H. Yang *et al.*, Programmed necrosis induced by asbestos in human mesothelial cells causes high-mobility group box 1 protein release and resultant inflammation. *Proc. Natl. Acad. Sci. U.S.A.* **107**, 12611–12616 (2010).
15. P. Scaffidi, T. Misteli, M. E. Bianchi, Release of chromatin protein HMGB1 by necrotic cells triggers inflammation. *Nature* **418**, 191–195 (2002).
16. S. Gardella *et al.*, The nuclear protein HMGB1 is secreted by monocytes via a non-classical, vesicle-mediated secretory pathway. *EMBO Rep.* **3**, 995–1001 (2002).
17. S. Jube *et al.*, Cancer cell secretion of the DAMP protein HMGB1 supports progression in malignant mesothelioma. *Cancer Res.* **72**, 3290–3301 (2012).
18. R. Mezzapelle *et al.*, Human malignant mesothelioma is recapitulated in immunocompetent BALB/c mice injected with murine AB cells. *Sci. Rep.* **6**, 22850 (2016).
19. G. Gaudino, J. Xue, H. Yang, How asbestos and other fibers cause mesothelioma. *Transl. Lung Cancer Res.* **9** (suppl. 1), S39–S46 (2020).
20. M. Carbone *et al.*, Biological mechanisms and clinical significance of *BAP1* mutations in human cancer. *Cancer Discov.* **10**, 1103–1120 (2020).
21. H. S. Lee, S. A. Lee, S. K. Hur, J. W. Seo, J. Kwon, Stabilization and targeting of INO80 to replication forks by BAP1 during normal DNA synthesis. *Nat. Commun.* **5**, 5128 (2014).
22. H. Yu *et al.*, Tumor suppressor and deubiquitinase BAP1 promotes DNA double-strand break repair. *Proc. Natl. Acad. Sci. U.S.A.* **111**, 285–290 (2014).
23. H. Yu *et al.*, The ubiquitin carboxyl hydrolase BAP1 forms a ternary complex with YY1 and HCF-1 and is a critical regulator of gene expression. *Mol. Cell. Biol.* **30**, 5071–5085 (2010).
24. E. Conway *et al.*, BAP1 enhances Polycomb repression by counteracting widespread H2AK119ub1 deposition and chromatin condensation. *Mol. Cell* **81**, 3526–3541.e8 (2021).
25. A. Bononi *et al.*, BAP1 regulates IP3R3-mediated Ca^{2+} flux to mitochondria suppressing cell transformation. *Nature* **546**, 549–553 (2017).
26. Y. Zhang *et al.*, BAP1 links metabolic regulation of ferroptosis to tumour suppression. *Nat. Cell Biol.* **20**, 1181–1192 (2018).
27. M. He *et al.*, Intrinsic apoptosis shapes the tumor spectrum linked to inactivation of the deubiquitinase BAP1. *Science* **364**, 283–285 (2019).
28. A. Bononi *et al.*, Germline BAP1 mutations induce a Warburg effect. *Cell Death Differ.* **24**, 1694–1704 (2017).
29. M. Carbone *et al.*, BAP1 and cancer. *Nat. Rev. Cancer* **13**, 153–159 (2013).
30. J. R. Testa *et al.*, Germline BAP1 mutations predispose to malignant mesothelioma. *Nat. Genet.* **43**, 1022–1025 (2011).
31. U. Andersson, K. J. Tracey, HMGB1 is a therapeutic target for sterile inflammation and infection. *Annu. Rev. Immunol.* **29**, 139–162 (2011).
32. B. Lu *et al.*, Novel role of PKR in inflammasome activation and HMGB1 release. *Nature* **488**, 670–674 (2012).
33. R. Sterner, G. Vidali, V. G. Allfrey, Studies of acetylation and deacetylation in high mobility group proteins. Identification of the sites of acetylation in HMG-1. *J. Biol. Chem.* **254**, 11577–11583 (1979).
34. C. Tabata *et al.*, Serum HMGB1 as a diagnostic marker for malignant peritoneal mesothelioma. *J. Clin. Gastroenterol.* **47**, 684–688 (2013).
35. H. I. Pass *et al.*, Characteristics of nine newly derived mesothelioma cell lines. *Ann. Thorac. Surg.* **59**, 835–844 (1995).
36. A. Napolitano *et al.*, Minimal asbestos exposure in germline BAP1 heterozygous mice is associated with deregulated inflammatory response and increased risk of mesothelioma. *Oncogene* **35**, 1996–2002 (2016).
37. M. Carbone *et al.*, Erionite exposure in North Dakota and Turkish villages with mesothelioma. *Proc. Natl. Acad. Sci. U.S.A.* **108**, 13618–13623 (2011).
38. F. Qi *et al.*, Continuous exposure to chrysotile asbestos can cause transformation of human mesothelial cells via HMGB1 and TNF-α signaling. *Am. J. Pathol.* **183**, 1654–1666 (2013).
39. L. Ulloa *et al.*, Ethyl pyruvate prevents lethality in mice with established lethal sepsis and systemic inflammation. *Proc. Natl. Acad. Sci. U.S.A.* **99**, 12351–12356 (2002).
40. L. Pellegrini *et al.*, HMGB1 targeting by ethyl pyruvate suppresses malignant phenotype of human mesothelioma. *Oncotarget* **8**, 22649–22661 (2017).
41. H. W. Choi *et al.*, Aspirin's active metabolite salicylic acid targets high mobility group box 1 to modulate inflammatory responses. *Mol. Med.* **21**, 526–535 (2015).
42. H. Xin *et al.*, HMGB1 increases radiosensitivity by interacting with HDAC1. *Chin. J. Radiol. Med. Prot.* **35**, 8–14 (2015).
43. M. J. McCauley, J. Zimmerman, L. J. Maher, 3rd, M. C. Williams, HMGB binding to DNA: Single and double box motifs. *J. Mol. Biol.* **374**, 993–1004 (2007).
44. X. Li, H. Yang, S. Huang, Y. Qiu, Histone deacetylase 1 and p300 can directly associate with chromatin and compete for binding in a mutually exclusive manner. *PLoS One* **9**, e94523 (2014).
45. F. Brambilla *et al.*, Nucleosomes effectively shield DNA from radiation damage in living cells. *Nucleic Acids Res.* **48**, 8993–9006 (2020).
46. H. Yang *et al.*, Aspirin delays mesothelioma growth by inhibiting HMGB1-mediated tumor progression. *Cell Death Dis.* **6**, e1786 (2015).
47. S. Pastorino *et al.*, A subset of mesotheliomas with improved survival occurring in carriers of BAP1 and other germline mutations. *J. Clin. Oncol.* **36**, JCO2018790352 (2018).
48. M. Nasu *et al.*, High incidence of somatic BAP1 alterations in sporadic malignant mesothelioma. *J. Thorac. Oncol.* **10**, 565–576 (2015).
49. Y. Yoshikawa *et al.*, High-density array-CGH with targeted NGS unmask multiple noncontiguous minute deletions on chromosome 3p21 in mesothelioma. *Proc. Natl. Acad. Sci. U.S.A.* **113**, 13432–13437 (2016).
50. L. M. Krug *et al.*, Vorinostat in patients with advanced malignant pleural mesothelioma who have progressed on previous chemotherapy (VANTAGE-014): A phase 3, double-blind, randomised, placebo-controlled trial. *Lancet Oncol.* **16**, 447–456 (2015).
51. M. Carbone, G. Klein, J. Gruber, M. Wong, Modern criteria to establish human cancer etiology. *Cancer Res.* **64**, 5518–5524 (2004).
52. E. P. Henske, S. Jóźwiak, J. C. Kingswood, J. R. Sampson, E. A. Thiele, Tuberous sclerosis complex. *Nat. Rev. Dis. Primers* **2**, 16035 (2016).
53. J. E. Ellerman *et al.*, Masquerader: High mobility group box-1 and cancer. *Clin. Cancer Res.* **13**, 2836–2848 (2007).
54. T. Bald *et al.*, Ultraviolet-radiation-induced inflammation promotes angiotropism and metastasis in melanoma. *Nature* **507**, 109–113 (2014).
55. H. W. Chung *et al.*, Serum high mobility group box-1 is a powerful diagnostic and prognostic biomarker for pancreatic ductal adenocarcinoma. *Cancer Sci.* **103**, 1714–1721 (2012).
56. H. Lee *et al.*, Diagnostic significance of serum HMGB1 in colorectal carcinomas. *PLoS One* **7**, e34318 (2012).
57. M. Bocchetta *et al.*, Human mesothelial cells are unusually susceptible to simian virus 40-mediated transformation and asbestos cocarcinogenicity. *Proc. Natl. Acad. Sci. U.S.A.* **97**, 10214–10219 (2000).
58. A. Davtyan *et al.*, AWSEM-MD: Protein structure prediction using coarse-grained physical potentials and bioinformatically based local structure biasing. *J. Phys. Chem. B* **116**, 8494–8503 (2012).
59. M. Chen, X. Lin, W. Lu, J. N. Onuchic, P. G. Wolynes, Protein folding and structure prediction from the ground up II: AAWSEM for α/β proteins. *J. Phys. Chem. B* **121**, 3473–3482 (2017).
60. Y. Yan, D. Zhang, P. Zhou, B. Li, S. Y. Huang, HDOCK: A web server for protein-protein and protein-DNA/RNA docking based on a hybrid strategy. *Nucleic Acids Res.* **45** (W1), W365–W373 (2017).